

STRESS CONCENTRATION ANALYSIS IN ORTHOTROPIC PLATES

Lucas Lisbôa Vignoli¹

Jaime Tupiassú Pinho de Castro²

Marco Antonio Meggiolaro³

Department of Mechanical Engineering, Pontifical Catholic University of Rio de Janeiro, Rua Marques de Sao Vicente 225 - Gavea, Rio de Janeiro, RJ 22453-900

¹lucaslvig@gmail.com

²jtcastro@puc-rio.br

³meggi@puc-rio.br

Abstract. *Anisotropic materials are widely used for different industrial applications. An important class of anisotropic materials is the orthotropic one. Nine constants are necessary to characterize the elastic response of general orthotropic materials to mechanical loads, but thin composite plates can be approximately described using the plane stress assumption, which requires only four material constants. Even though the plane stress hypothesis seems to be quite restrictive, it can be used to model structural components made of plate-like panels, which are very common in practice. However, since most such components must have holes, slots, grooves, shoulders, corners, reinforcements, or similar abrupt geometric transitions generically called notches, the stress concentration problem in orthotropic plates has a major practical importance. This paper uses theoretical and numerical approaches to study stress concentration effects in orthotropic plates submitted to tension loads with an elliptical or circular hole. The theoretical part is developed using the well-established Stroh formalism for infinite plates. The numerical part is implemented and solved using the ANSYS commercial finite element package. The focus of the FE analysis is to evaluate the stress distribution along the hole border for finite plates. The results are compared to the classical analysis for isotropic materials for both finite and infinite plates, as well as to some approximate methods to estimate stress concentration effects for finite orthotropic plates.*

Keywords: *stress concentration, orthotropic plates, Stroh formalism*

1. INTRODUCTION

Abrupt geometric variations generically called notches are unavoidable in real structures. The stress field near the tips of such notches can be much higher than it would be if the notch was not there, an effect known as stress concentration (SC). Therefore, such notch tips usually are critical points for structural analysis purposes. So far, just few cases of SC have analytical solution; most of them for holes in infinite plates made of isotropic materials.

The use of anisotropic materials is increasing at a growing rate in industrial applications since the middle of the last century, especially for composite and monocrystal components. The possibility to join lightweight with high strength, e.g. in aeronautical applications, or to operate in very high temperatures, e.g. in heat engines (monocrystals are especially important for gas turbines blades and vanes, since they maximize their creep resistance), are characteristics that make composite structures so popular.

Therefore, the study of stress concentration problems in anisotropic materials has an increasing importance for structural engineers as well. However, they cannot be treated as simple extensions of the corresponding isotropic problems. For instance, for the specific composite studied in this paper, the maximum and minimum values of the stress along the notch boundary in an infinite plate with a circular hole subjected to unidirectional traction load is around seven and minus seven, while for the same problem in an isotropic material these values are three and minus one. This means that the use of an isotropic stress concentration factor to design or analyze an anisotropic component can lead to severe *non-conservative* errors, a totally unacceptable procedure in practical applications, as discussed next.

2. ANALYTICAL APPROACH

Kirsch was the first to calculate the stress distribution around a circular hole in an infinite plate, and Inglis solved some years later the SC problem for elliptical holes (Castro and Meggiolaro, 2009). Muskhelishvili (1977) introduced complex stress functions that can be used to solve many stress analysis problems, and using them Savin (1970) wrote a comprehensive book on the solution of SC problems.

Generalizing the Muskhelishvili solution technique for orthotropic materials, Lekhnetskii (1981, 1987), made important contributions to the Theory of Elasticity of anisotropic bodies, introducing a solution method known as Lekhnetskii formalism. However, Lekhnetskii formalism is mathematically difficult and is not able to solve the general

anisotropic material problem. Stroh formalism (Ting, 1996) is an elegant, powerful, simpler method to attack such problems, and because of this it is the preferential approach used in this paper. A brief overview about the elasticity formulations for anisotropic materials and some approximations are presented by Sevenois and Koussios (2014).

For the analytical part of this paper, two steps are considered: the stress and strain distributions using theory of elasticity for anisotropic plates in generalized plane stress conditions using the Stroh formalism, and the application of failure criteria to estimate their strength using the Tsai's method (1988).

2.1 Anisotropic Theory of Elasticity

Due to space limitations, only the stress distribution along the hole boundary for general plane stress condition using Stroh formalism based in Ting (1996) and Hwu (2009) is presented here. For a detailed deduction, the same references might be consulted. First of all, the system of coordinates used in this paper is introduced in Fig.1.

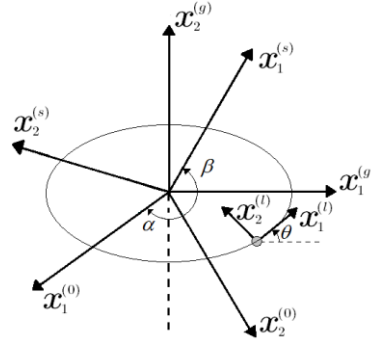


Figure 1. Coordinate system

For a general case of anisotropy for a bi-dimensional plate, four sets of axes are necessary: $x_i^{(0)}$ are used to define the material properties; $x_i^{(s)}$ coincide with the ellipse semi-axes direction; $x_i^{(l)}$ are used to map the hole border; the load is applied in $x_i^{(s)}$. The load can be transferred from $x_i^{(s)}$ to $x_i^{(g)}$ using Mohr's circle as (Crandall et al., 1978)

$$\sigma_{11}^{(g)} = \left(\frac{\sigma_{11}^{(s)} + \sigma_{22}^{(s)}}{2} \right) + \left(\frac{\sigma_{11}^{(s)} - \sigma_{22}^{(s)}}{2} \right) \cos(2\beta) - \sigma_{12}^{(s)} \sin(2\beta) \quad (1.a)$$

$$\sigma_{22}^{(g)} = \left(\frac{\sigma_{11}^{(s)} + \sigma_{22}^{(s)}}{2} \right) - \left(\frac{\sigma_{11}^{(s)} - \sigma_{22}^{(s)}}{2} \right) \cos(2\beta) + \sigma_{12}^{(s)} \sin(2\beta) \quad (1.b)$$

$$\sigma_{12}^{(g)} = \left(\frac{\sigma_{11}^{(s)} - \sigma_{22}^{(s)}}{2} \right) \sin(2\beta) + \sigma_{12}^{(s)} \cos(2\beta) \quad (1.c)$$

It is important to emphasize that the loads $\sigma_{ij}^{(s)}$ are applied very far from the notch border. Once the stresses are obtained at the global axes, the following stress vectors are conveniently defined

$$\tau_1^{(g)} = \begin{bmatrix} \sigma_{11}^{(g)} \\ \sigma_{12}^{(g)} \\ 0 \end{bmatrix} \quad \tau_2^{(g)} = \begin{bmatrix} \sigma_{12}^{(g)} \\ \sigma_{22}^{(g)} \\ 0 \end{bmatrix} \quad (2)$$

As in any elasticity problem, geometric compatibility, constitutive relations, and equilibrium conditions are the basis for the solution. For the Stroh formalism it must not be different, and they are expressed using the index notation as (body force are not considered)

$$\varepsilon_{ij}^{(l)} = \frac{1}{2} (u_{i,j}^{(l)} + u_{j,i}^{(l)}) \quad (3.a)$$

$$\sigma_{ij}^{(l)} = c_{ijkl}^{(l)} \varepsilon_{kl}^{(l)} = c_{ijkl}^{(l)} u_{k,l}^{(l)} \quad (3.b)$$

$$\sigma_{ij,j}^{(l)} = c_{ijkl}^{(l)} u_{k,lj}^{(l)} = 0 \quad (3.c)$$

where u_i and ε_{ij} denote the displacement and strain components and $c_{ijkl}^{(l)}$ is the stiffness matrix in local coordinate.

Before the next step, a notation issue should be commented: in this text, capital letters are used to represent matrix notation and lower cases for the index one. Thus considering an orthotropic material, the compliance matrices defined on the coordinates $x_i^{(0)}$ and $x_i^{(l)}$ are

$$s^{(0)} = \begin{bmatrix} \frac{1}{E_1} & -\frac{\nu_{12}}{E_1} & 0 \\ -\frac{\nu_{12}}{E_1} & \frac{1}{E_2} & 0 \\ 0 & 0 & \frac{1}{G_{12}} \end{bmatrix} \quad s^{(l)} = \begin{bmatrix} \frac{1}{E_1^{(l)}} & -\frac{\nu_{12}^{(l)}}{E_1^{(l)}} & \frac{\eta_{12,1}^{(l)}}{E_1^{(l)}} \\ \frac{\nu_{12}^{(l)}}{E_1^{(l)}} & \frac{1}{E_2^{(l)}} & \frac{\eta_{12,2}^{(l)}}{E_2^{(l)}} \\ \frac{\eta_{12,1}^{(l)}}{E_1^{(l)}} & \frac{\eta_{12,2}^{(l)}}{E_2^{(l)}} & \frac{1}{G_{12}^{(l)}} \end{bmatrix} \quad (4)$$

The materials properties in the $x_i^{(l)}$ system are obtained from the following relations

$$E_1^{(l)} = \left[\frac{\cos^4(\theta + \alpha)}{E_1} + \left(\frac{1}{G_{12}} - \frac{2\nu_{12}}{E_1} \right) \cos^2(\theta + \alpha) \sin^2(\theta + \alpha) + \frac{\sin^4(\theta + \alpha)}{E_2} \right]^{-1} \quad (5.a)$$

$$E_2^{(l)} = \left[\frac{\sin^4(\theta + \alpha)}{E_1} + \left(\frac{1}{G_{12}} - \frac{2\nu_{12}}{E_1} \right) \cos^2(\theta + \alpha) \sin^2(\theta + \alpha) + \frac{\cos^4(\theta + \alpha)}{E_2} \right]^{-1} \quad (5.b)$$

$$G_{12}^{(l)} = \left[\frac{1}{G_{12}} + \left(\frac{1 + \nu_{12}}{E_1} + \frac{1 + \nu_{21}}{E_2} - \frac{1}{G_{12}} \right) \sin^2 2(\theta + \alpha) \right]^{-1} \quad (5.c)$$

$$\nu_{12}^{(l)} = E_1 \left[\frac{\nu_{12}}{E_1} - \frac{1}{4} \left(\frac{1 + \nu_{12}}{E_2} + \frac{1 + \nu_{21}}{E_2} - \frac{1}{G_{12}} \right) \sin^2 2(\theta + \alpha) \right] \quad (5.d)$$

$$\eta_{12,1}^{(l)} = E_1 \left[\frac{\sin^2(\theta + \alpha)}{E_2} - \frac{\cos^2(\theta + \alpha)}{E_1} + \frac{1}{2} \left(\frac{1}{G_{12}} - \frac{2\nu_{12}}{E_1} \right) \cos 2(\theta + \alpha) \right] \sin 2(\theta + \alpha) \quad (5.e)$$

$$\eta_{21,2}^{(l)} = E_2 \left[\frac{\cos^2(\theta + \alpha)}{E_2} - \frac{\sin^2(\theta + \alpha)}{E_1} - \frac{1}{2} \left(\frac{1}{G_{12}} - \frac{2\nu_{12}}{E_1} \right) \cos 2(\theta + \alpha) \right] \sin 2(\theta + \alpha) \quad (5.f)$$

Once the compliance matrices are obtained, the stiffness matrices can be computed using the inverse relation.

Assuming that no pressure is acting inside the hole, the stress component $\sigma_{22}^{(l)}$ must be zero along the hole border and the stress vectors are completely defined, in other words, the stress at the infinite are known (prescribed), $\sigma_{11}^{(l)}$ is expressed as

$$\sigma_{11}^{(l)} = i_1^T \left[G_1^{(l)} \tau_2^{(g)} + \frac{b}{a} G_3^{(l)} \tau_1^{(g)} \right] - i_2^T \left[G_1^{(l)} \tau_1^{(g)} - \frac{a}{b} G_3^{(l)} \tau_2^{(g)} \right] \quad (9)$$

where $i_1^T = (1 \ 0 \ 0)$ and $i_2^T = (1 \ 0 \ 0)$ are unit vectors used to decompose the stress vector components, $G_1^{(l)} = [N_1^{(l)}]^T - N_3^{(l)} S^{bl} (L^{bl})^{-1}$ and $G_3^{(l)} = -N_3^{(l)} (L^{bl})^{-1}$ are two real matrices defined to abbreviate the final result, $N_1^{(l)} = -[T^{(l)}]^{-1} [R^{(l)}]^T$ and $N_3^{(l)} = R^{(l)} [T^{(l)}]^{-1} [R^{(l)}]^T - Q^{(l)}$ are components of the fundamental elasticity matrix and $S^{bl} = \frac{1}{\pi} \int_0^\pi N_1^{(l)} d\theta$ and

$L^{bl} = -\frac{1}{\pi} \int_0^\pi N_3^{(l)} d\theta$ are the Barnett–Lothe tensors. Note the superscript bl to denote the Barnett–Lothe tensors. A useful

explicit equation for the Barnett-Lothe tensor for plane stress condition for orthotropic materials is (Ting, 1996)

$$S^{bl} = \begin{bmatrix} 0 & S_{12}^{bl} & 0 \\ S_{21}^{bl} & 0 & 0 \\ 0 & 0 & 0 \end{bmatrix} \quad L^{bl} = \begin{bmatrix} L_{11}^{bl} & 0 & 0 \\ 0 & L_{22}^{bl} & 0 \\ 0 & 0 & L_{33}^{bl} \end{bmatrix} \quad (10)$$

where

$$S_{12}^{bl} = \left[\left(\frac{E_2}{G_{12}} \right) + 2 \frac{1 - \sqrt{\nu_{12}\nu_{21}}}{\sqrt{\frac{E_2}{E_1}}} \right]^{-1/2} \frac{1 - \sqrt{\nu_{12}\nu_{21}}}{\sqrt{\frac{E_2}{E_1}}} \quad (11.a)$$

$$S_{21}^{bl} = - \frac{\left[\left(\frac{E_1}{G_{12}} \right) + 2 \frac{1 - \sqrt{\nu_{12}\nu_{21}}}{\sqrt{\frac{E_1}{E_2}}} \right]^{-1/2}}{\left[\left(\frac{E_2}{G_{12}} \right) + 2 \frac{1 - \sqrt{\nu_{12}\nu_{21}}}{\sqrt{\frac{E_2}{E_1}}} \right]^{-1/2}} \left[\left(\frac{E_2}{G_{12}} \right) + 2 \frac{1 - \sqrt{\nu_{12}\nu_{21}}}{\sqrt{\frac{E_2}{E_1}}} \right]^{-1/2} \frac{1 - \sqrt{\nu_{12}\nu_{21}}}{\sqrt{\frac{E_2}{E_1}}} \quad (11.b)$$

$$L_{11}^{bl} = \left[\frac{E_1}{1 - \sqrt{\nu_{12}\nu_{21}}} \right] \left[\left(\frac{E_2}{G_{12}} \right) + 2 \frac{1 - \sqrt{\nu_{12}\nu_{21}}}{\sqrt{\frac{E_2}{E_1}}} \right]^{-1/2} \frac{1 - \sqrt{\nu_{12}\nu_{21}}}{\sqrt{\frac{E_2}{E_1}}} \quad (11.c)$$

$$L_{22}^{bl} = - \left[\frac{E_1}{1 - \sqrt{\nu_{12}\nu_{21}}} \right] \frac{\left[\left(\frac{E_1}{G_{12}} \right) + 2 \frac{1 - \sqrt{\nu_{12}\nu_{21}}}{\sqrt{\frac{E_1}{E_2}}} \right]^{-1/2}}{\left[\left(\frac{E_2}{G_{12}} \right) + 2 \frac{1 - \sqrt{\nu_{12}\nu_{21}}}{\sqrt{\frac{E_2}{E_1}}} \right]^{-1/2}} \left[\left(\frac{E_2}{G_{12}} \right) + 2 \frac{1 - \sqrt{\nu_{12}\nu_{21}}}{\sqrt{\frac{E_2}{E_1}}} \right]^{-1/2} \frac{1 - \sqrt{\nu_{12}\nu_{21}}}{\sqrt{\frac{E_2}{E_1}}} \quad (11.d)$$

$$L_{33}^{bl} = \sqrt{G_{13}G_{23}} \quad (11.e)$$

Despite G_{13} and G_{23} appear on the result, as the matrices are multiplied by the unit vector at the final expression, that has the same effect of a dot product, these terms are eliminated.

2.2 Failure Theories

Failure criterion is an issue for anisotropic materials, especially for composites. Because of it, a global effort has been happen to evaluate the existent theories applied to fiber reinforced polymer composite and is known as World-Wide Failure Exercise (WWFE). The first WWFE is already finished and many criterions were tested, but some doubts still remained and the second and third WWFE, so the final results are not available. The recommendations and conclusions of the first WWFE, as well as all the paper published in this exercise, are compiled in one book (Hinton et al., 2004), whose results are used bellow.

Five failure theories stood out between the seventeen tested: Zinoviev's; Tsai's; Puck's; Bogetti's; and Cuntze's. Each one has advantages and disadvantages, so none of them is the best in consensus. For this paper, Tsai's theory was chosen because is the most widely adopted. This theory is also known as Quadratic failure criterion and is purely empirical. Considering the stress components acting the coordinate system aligned to the fiber direction, $x_i^{(0)}$, the function which describe the failure is

$$f_{Tsai} = \frac{\sigma_{11}^{(0)2}}{X_{11}^t X_{11}^c} + F_{12}^* \frac{\sigma_{11}^{(0)} \sigma_{22}^{(0)}}{\sqrt{X_{11}^t X_{11}^c X_{22}^t X_{22}^c}} + \frac{\sigma_{22}^{(0)2}}{X_{22}^t X_{22}^c} + \left(\frac{\sigma_{12}^{(0)}}{X_{12}^s} \right)^2 + \left(\frac{1}{X_{11}^t} - \frac{1}{X_{11}^c} \right) \sigma_{11}^{(0)} + \left(\frac{1}{X_{22}^t} - \frac{1}{X_{22}^c} \right) \sigma_{22}^{(0)} \quad (12)$$

Where X_{ij}^t , X_{ij}^c and X_{ij}^s denote strength related to the load $\sigma_{ij}^{(0)}$ and the superscripts "t", "c" and "s" means tension, compression and shear and F_{12}^* is used to quantify the interaction between stresses $\sigma_{11}^{(0)}$ and $\sigma_{22}^{(0)}$ during the failure (a common value is $F_{12}^* = -0.5$). Failure takes place when $f_{Tsai} = 1$.

3. FINITE ELEMENT MODEL

This section present FE models made using the ANSYS commercial package for five different plates with a circular hole loaded under uniaxial tension along the $x_l^{(g)}$ direction. The difference between the plates is the ratio hole diameter to plate width. Ratios 0.1, 0.2, 0.3, 0.4 and 0.5 are used. One orthotropic material is selected to be used and to evaluate the influence of the stress distribution according to the angle α defined in Fig.1, four different values of these angle for each plate will be simulated: 0°, 30°, 60° and 90°. The hole diameter and the plate length are fixed for all simulations, 1mm and 30mm, respectively. To avoid repetitive information, just one mesh is presented in Fig. 2 for the plate with ratio hole diameter to plate width equal to 0.3, albeit some small changes of the mesh were applied for the other ones; basically the element size used was smaller or larger for the thinner or wider plates.

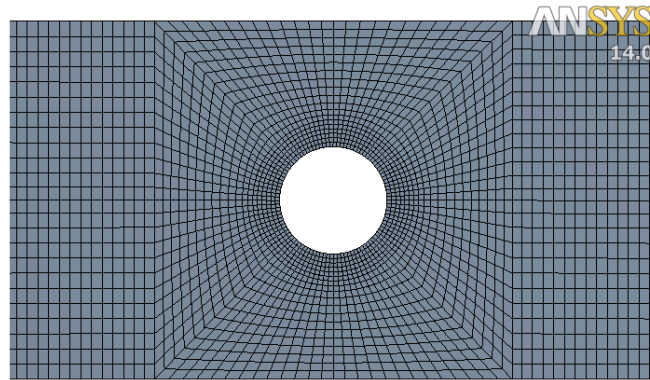


Figure 2. Mesh generate for the FE model.

The geometry was split in three different groups to apply the mesh: an inner circular part, where the element size was kept constant to guarantee the stress convergence near the perturbed region; a semi-square part to connect smoothly the circular part to the other part of the plate (note that in this region the element size is growing); and the outer part of the plate, where the horizontal length is tending to infinity size (in this one the element size is constant). Elements PLANE183 and SURF153 were used. PLANE183 is a quadrilateral higher order element with 8 nodes and SURF153 is used for load application. For a detailed description of the elements formulations, see Ansys (2009).

3.1 Problems with symmetry conditions

One-quarter symmetry can be adopted to simulate stress concentration problems for a circular hole in isotropic plates, but for anisotropic plates the one-quarter symmetry becomes invalid because the periodicity of the stress distribution is 180° , not 90° . One-half symmetry could be a possibility to decrease computation cost, but as can be noted in Fig.3, this also do not represent the real stress distributions for any α different of 0° or 90° because a continuity issue takes place.

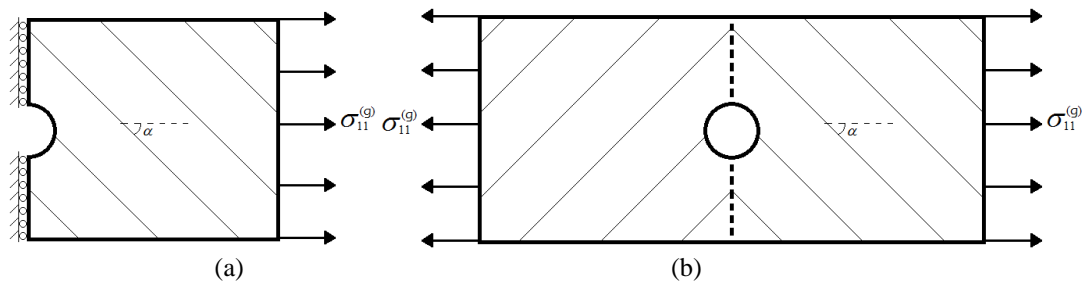


Figure 3. Symmetry representations: (a) boundary condition of the one-half model; (b) continuity issue representation.

To illustrate the error generated when symmetry is used, one simulation using the one-half geometry for the plate with $\alpha = 60^\circ$ and is presented in the next section.

4. APPLICATIONS

To illustrate the applications of the analytical and of the FE model presented in this paper, an orthotropic composite material with carbon fiber (AS4) is used. Its mechanical properties (see Table 1) are taken from Hinton et al., 2004. To compare the differences of the stress distribution, an isotropic set of properties (Table 1) is used as well (Castro and Meggiolaro, 2009). The materials properties are not necessary to evaluate the stress distribution for isotropic materials, so as the goal of this paper is to use the Stroh formalism, just two (independent) properties are necessary.

With these mechanical properties, the analytical result for unidirectional stress $\sigma_{11}^{(g)}$ is applied for a range of α and θ between 0° and 180° . These ranges are used to represent the periodicity of the function. In this section the Stress Concentration Factor (SCF) will be used to present the results. The results are plotted in Fig.4.

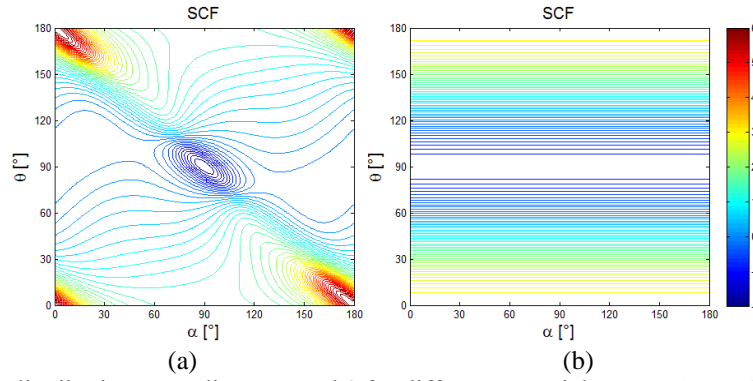


Figure 4. SCF distribution according to α and θ for different materials: (a) orthotropic; (b) isotropic.

Note that both Fig.(a) and Fig.(b) in Fig.4 are plotted with the same color scale. The value of α can be chosen and for each possible value of α , θ can vary from 0° to 180° and as it must be, the stress distribution do not depend on α for isotropic materials. Another important conclusion from these results is that the point of maximum and minimum tangential stress is not constant for orthotropic materials, unlike the isotropic.

Table 1. Material properties using to evaluate both models.

Material Properties	Orthotropic (Composite - AS4)	Isotropic (Structural Steel)
Longitudinal Modulus [GPa] - E_1	126	205
Transverse Modulus [GPa] - E_2	11	-
Major Poisson's Ratio - ν_{12}	0.28	0.29
In-plane Shear Modulus [GPa] - G_{12}	6.6	-
Longitudinal Tensile Strength [MPa] - X_{11}^t	1950	-
Longitudinal Compressive Strength [MPa] - X_{11}^c	1480	-
Transverse Tensile Strength [MPa] - X_{22}^t	48	-
Transverse Compressive Strength [MPa] - X_{22}^c	200	-
In-plane Shear Strength [MPa] - X_{12}^s	70	-

Another interesting result that can be obtained analyzing Eq. 4 is that the tangential stress produces shear strains for $(\alpha + \theta)$ different from 90° or any integer multiplied by 90° , including 0. From this fact, the direction of the principal strains can be calculated as (Crandall et al., 1978)

$$\phi_{strain} = \frac{1}{2} a \tan \left(\frac{2\varepsilon_{12}^{(l)}}{\varepsilon_{11}^{(l)} - \varepsilon_{22}^{(l)}} \right) \quad (13)$$

And for the same load condition, material (orthotropic) and α and θ ranges, the principal strain direction is presented in Fig.5.a. It results in an important point for fatigue analysis. For isotropic materials, the principal stresses and principal strains directions are coincident, hence it makes no difference to think that cracks that appear on the direction of maximum shear stress/strain propagate perpendicular to the maximum normal stress/strain direction. However, for anisotropic materials two different possible directions of crack initiation, as well as two different directions of crack propagation, should be evaluated.

For general biaxial load for the analytical approach presented in section 2, the maximum tangential stress and the maximum Tsai's function are computed for a range of α from 0° to 180° . A routine was implemented using MATLAB to evaluate the maximum value of each α , varying θ , and saving this value in a matrix. The results are in Fig. 5.b and 5.c.

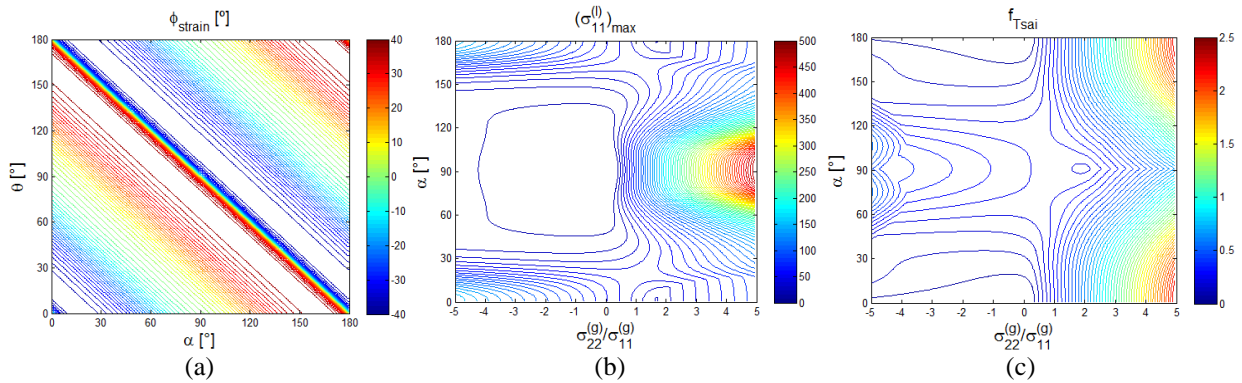


Figure 5: (a) Principal strain direction for the orthotropic material; and Maximum value for a range of α in biaxial load: (b) tangential stress; (c) Tsai's failure criterion.

Figure 5 shows the influence of α during the design step and that to minimize the stress concentration may not be the most important thing for anisotropic materials. Sometimes to minimize Tsai's function (or any other failure criterion) is more important.

Figure 6 shows the FE results of the SCF distribution for different values of α . Note that the SCF is compared with the gross area, despite it is more common to use the net area, for anisotropic material it becomes more conveniently use the gross area because the distribution of the SC along the whole hole edge is desired. Most of the analytical finite plates studies in the literature consider that the stress distribution shape do no change with the variation when the plate width decreases. This assumption is not true; however, analyzing the FE results in Fig.6, it is possible to realize that this is a reasonable hypothesis.

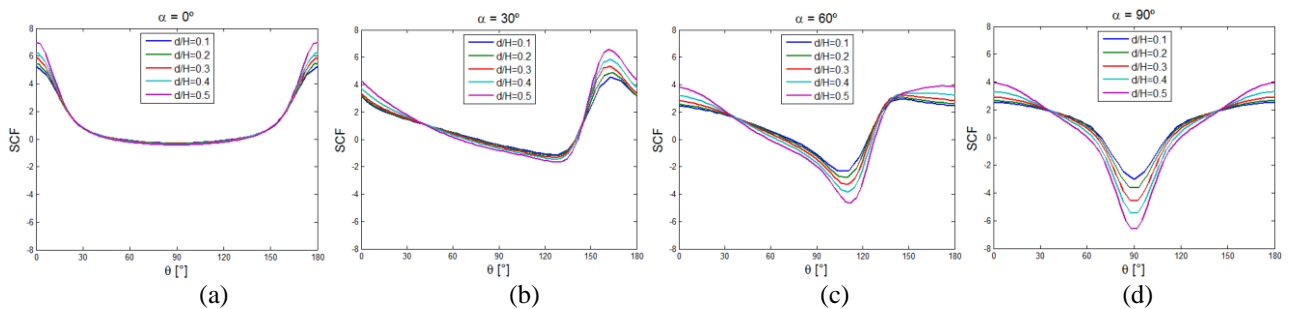


Figure 6. SCF distribution for different values of α . (a) $\alpha=0^\circ$; (b) $\alpha=30^\circ$; (c) $\alpha=60^\circ$; (d) $\alpha=90^\circ$.

Tan, 1987 and 1988, presented a study about the influence of holes in finite plates in orthotropic materials and proposed a popular formula to approximate the SCF for circular and elliptical holes (for elliptical holes the major semi-axis is perpendicular to the load direction). Zappalorto and Carraro, 2015, proposed an analytical formulation, based in numerical and experimental results, to estimate the SCC factor orthotropic plates subjected tension loads considering hyperbolic and elliptical notches. Both formulations give an approximation for a maximum value of SCF instead the whole distribution and do not consider that the maximum SCF can be not at the same point that it would be for isotropic plate, what limits their application.

Before conclude the results presentation, one final FE element analysis was carried out, as explained in section 3.2. Two additional dotted lines are added to the result of the SCF distribution: the SCF's for $\theta = 0^\circ$ and for $\theta = 90^\circ$. Figure 7 gives a clear explanation for how to consider the symmetry condition at the FE model.

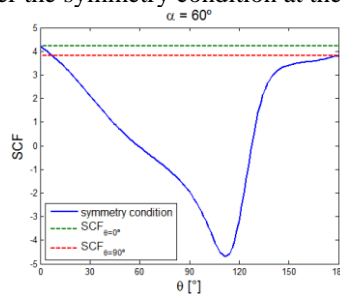


Figure 7. Example of error generate in use symmetry condition for anisotropic material.

Pedersen, et al., 1992, and Cho and Rowlands, 2009, carried out numerical investigations about optimization of fiber directions for composite materials. Despite different approaches, both used one quarter symmetry condition and no

consideration about the possibility of error generated because this boundary condition was done. It must be clear that the analytical solution is symmetric for each 180°, what becomes even worst the use of one quarter of the plate, besides the physical interpretation presented in Fig. 3.

5. CONCLUSION

A brief review of the Stroh formalism was presented considering the case of orthotropic materials with an elliptical hole. Before use the final equation it is important to keep in mind the load direction, as well as the direction where the materials are defined, because of it four coordinates system were used.

Once the stress distribution along the hole border is obtained, a failure criterion is applied to verify the influence of the fibers directions at the stress level and the strength of the arrangement. An important result presented is that for certain biaxial ratio load, the fibers position which gives the maximum value of stress offers the maximum strength, in other words, a given fiber position can maximize the stress and minimize the Tsai's function at the same time. It becomes clear for $\sigma_{22}^{(g)}/\sigma_{11}^{(g)} = 5$ and $\alpha = 90^\circ$, thus it should not be emphasized to minimize the stress but the ratio stress/strength according to the failure criterion.

The presented FE model uses no symmetry condition, because as proved, no symmetry can be used for applying the boundary conditions. The numerical approach has the aim to study finite plates and shows that the assumption used for some authors to consider the stress distribution shape along the border the same independently of the ratio between hole diameter and plate width is a good hypothesis.

Another important point presented here is the difference between the principal stress and strain directions, which is important especially for fatigue and fracture mechanics. Both directions are coincident for isotropic materials, but this is not true for anisotropic materials.

6. ACKNOWLEDGEMENTS

The authors thank the Brazilian foundation CNPq and the PUC-Rio for financial support.

7. REFERENCES

- Anslys, 2009. *Theory Reference for the Mechanical APDL and Mechanical Applications*.
- Castro, J.T.P., Meggiolaro, M.A., 2009. *Fadiga – Técnicas Práticas de Dimensionamento Estrutural sob Cargas Reais de Serviço – Volume I – Iniciação de Trincas*, Amazon Books.
- Cho, H.K., Rowlands, R.E., 2009. "Optimizing Fiber Direction in Perforated Orthotropic Media to Reduce Stress Concentration", *Journal of Composite Materials*, Vol. 43, n. 10, p. 1177-1198.
- Crandall, S. H., Dahl, N. C., Lardner, T. J., 1978. *An Introduction to the Mechanics of Solids*, 2nd Ed., McGraw-Hill.
- Hinton, M.J., Kaddour, A.S., Soden, P.D., 2004. *Failure Criteria in Fibre Reinforced Polymer Composites: The World-Wide Failure Exercise*, Elsevier.
- Hwu, C., 2009. *Anisotropic Elastic Plates*. Springer.
- Lekhniskii, S.G., 1987. *Anisotropic Plates*, 3rd Ed., Gordon and Breach Science Publishers.
- Lekhniskii, S.G., 1981. *Theory of Elasticity of an Anisotropic Body*, Mir.
- Muskhelishvili, N.I., 1977, *Some Basic Problems of the Mathematical Theory of Elasticity*, Springer.
- Pedersen, P., Tobiesen, L., Jensen, S.H., 1992. "Shapes of Orthotropic Plates for Minimum Energy Concentration", *Mech. Struct. & Mach.*, Vol. 20(4), p. 499-514.
- Savin, G. N., 1970. *Stress Distribution Around Holes*, NASA Technical Translation.
- Sevenois, R. D. B., Koussios, S., 2014. "Analytic Methods for Stress Analysis of Two-Dimensional Flat Anisotropic Plates With Notches: An Overview", *Appl. Mech. Rev.*, Vol. 66(6), p. 060802.
- Tan, S.C., 1987. "Laminated Composites Containing an Elliptical Opening. I. Approximate Stress Analyses and Fracture Models", *Journal of Composite Materials*, Vol. 21, n. 10, p. 925-948 .
- Tan, S.C., 1988, "Finite-Width Correction Factors for Anisotropic Plate Containing a Central Opening", *Journal of Composite Materials*, Vol. 22, n. 11, p. 1080-1097.
- Ting, T.C.T., 1996. *Anisotropic Elasticity: Theory and Applications*, Oxford University Press.
- Tsai, S.W., 1988. *Composites Design*, 4th Ed., Think Composites.
- Zappalorto, M., Carraro, P.A., 2015. "An engineering formula for the stress concentration factor of orthotropic composite plates", *Composites: Part B*, Vol. 68, p. 51-58.

8. RESPONSIBILITY NOTICE

The authors are the only responsible for the printed material included in this paper.